Analytica Chimica Acta xxx (2018) 1–6

Contents lists available at ScienceDirect

Analytica Chimica Acta

journal homepage: www.elsevier.com/locate/aca

Platinum-loaded mesoporous nickel phosphonate and its electrochemical application for sarcosine detection

Qia Wang, Chun Yang, Qingui Yang, Shenghao Yu, Haipeng Yang*

College of Materials Science and Engineering, Shenzhen Key Laboratory of Polymer Science and Technology, and Guangdong Research Center for Interfacial Engineering of Functional Materials, Shenzhen University, Shenzhen, Guangdong, 518060, People's Republic of China

HIGHLIGHTS

- Synthesis of platinum-loaded mesoporous nickel phosphonate.
- Electrochemical detection of sarcosine with a low LOD of 0.24 μM.
- Good performance in the anti-interference test and in the real serum sample.

GRAPHICAL ABSTRACT

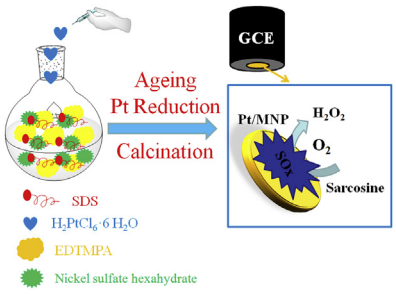

ARTICLE INFO

Article history:
Received 30 July 2018
Received in revised form
2 September 2018
Accepted 13 September 2018
Available online xxx

Keywords:
Mesoporous
Sarcosine biosensor
Nickel phosphonate
Platinum
Prostate cancer

ABSTRACT

In 2009, Sreekumar found that sarcosine, as an effective biomarker, can be used to identify prostate cancer. However, it is difficult to detect sarcosine in urine or plasma because of its low concentration. In this work, we describe a simple strategy for the preparation of sarcosine biosensor based on platinum-loaded mesoporous nickel phosphonate (Pt/MNP) and subsequently apply it to detect sarcosine. Mesoporous structure could increase the active sites on the MNP surface, which makes the Pt/MNP have excellent electrochemical performance for detecting hydrogen peroxide, one of the enzymatic products, and the sarcosine biosensor exhibited a superior electrochemical performance. The linear range of sarcosine biosensor is from 5 to 40 μM and the sensitivity is 123.51 μA mM^{-1} cm^{-2}. The limit of detection is estimated to be 0.24 μM (S/N = 3). Additionally, the sarcosine biosensor based on Pt/MNP also shows an excellent performance in the anti-interference test and the real serum sample. This work manifests the potential application of Pt/MNP as a novel biosensor material for sarcosine detection, which could be extended to other oxidase-based detection systems.

1. Introduction

Prostate cancer is one of the common malignant tumors in men, especially in those of over fifty years old, and its incidence increases greatly with age [1–3]. The incidence of prostate cancer is increasing in China, due to the improvement of living standards and the ageing of the population [1–4]. A man in the early stages of prostate cancer may not have any symptoms. Nevertheless, symptoms such as hematuria appeared while prostate cancer was likely to develop to its advanced stage [5,6]. So identifying prostate cancer in its early stages is significant for men's health, which contributes to reducing the rate of death from prostate cancer. At

* Corresponding author.
E-mail address: yanghp@szu.edu.cn (H. Yang).

https://doi.org/10.1016/j.aca.2018.09.027
0003-2670/

present, prostate cancer can be diagnosed mainly via digital rectal examination [7] and prostate specific antigen (PSA) test [8]. However, these methods do their limitations. Studies exhibited that there were numerous physiological and pathological factors, which influence the expression of PSA, so it resulted in a high false negative rate (15.2%) and false positive rate (30%), which will bring some trouble to the diagnosis of the disease [8–10]. Digital rectal examination requires doctors to have a wealth of clinical experience and it cannot make a detailed diagnosis of the tumor when volume of the tumor is relatively minor [10]. Therefore, new biomarkers which can quickly identify prostate cancer will make significant progress in the treatment of prostate cancer.

In 2009, Sreekumar et al. found that sarcosine was an effective biomarker to identify prostate cancer [11]. By detecting the concentration of sarcosine in urine or plasma, whether a patient has prostate cancer or not can be distinguished and it relieves patients from pain of prostate biopsy [10–12]. However, the detection of sarcosine is a tremendous challenge. For healthy male, sarcosine concentration is 102 and 139 ng mL^{-1} (about 1–1.5 μM) in serum and urine, respectively [13]. The concentration of sarcosine is so low that it cannot be easily detected [11,13]. Currently, the detection methods most used are electrochemiluminescence [14], fluorescence [15] and tandem mass spectrometry [10]. But unfortunately, these methods are not convenient and even have high medical cost to the patients. Simple and inexpensive way to detect sarcosine will greatly help the diagnosis of prostate cancer. Compared to the method mentioned above, the electrochemical method is simple and inexpensive. For example, nano Pt@ZIF8 modified electrode [16] and sarcosine oxidase composite screen-printed electrode [17] had been applied to detect sarcosine. They had achieved favorable results in the detection of sarcosine. The catalytic reaction process (Eq. (1)) [17] of sarcosine oxidase (SOx) is:

$$\text{Sarcosine} + O_2 + H_20 \overset{SOx}{\rightarrow} \text{Glycine} + \text{Formaldehyde} + H_2O_2 \quad (1)$$

These methods mainly utilize the specific catalytic ability of sarcosine oxidase to converse sarcosine to glycine, formaldehyde and hydrogen peroxide (H_2O_2), and detect one of its enzymatic products [17,18].

In this work, a sarcosine biosensor based on platinum-loaded mesoporous nickel phosphonate (Pt/MNP) was described. Pt/MNP was synthesized by hydrothermal synthesis method and in situ reduction of $PtCl_6^{2-}$ with a surfactant (Sodium dodecyl sulfate, SDS) as a soft template. Mesoporous structure could increase the active sites on the MNP surface, which makes the sarcosine biosensor exhibit a superior electrochemical performance [18,19]. Platinum, as a noble metal with high catalytic activity, not only has excellent electrochemical performance in H_2O_2, one of the oxidase enzymatic products, but also reduces the potential of electrochemical detection, which improves the anti-interference performance of the sarcosine biosensor [20–22]. The SOx was immobilized onto the surface of Pt/MNP/GCE by glutaraldehyde (GA) to obtain a sarcosine biosensor and afterward it was utilized to detect and analyze sarcosine. The sarcosine biosensor based on Pt/MNP exhibits excellent anti-interference and detection performance for sarcosine.

2. Experimental

2.1. Chemicals and reagents

Nickel sulfate hexahydrate was purchased from Sinopharm Chemical Reagent Co., Ltd. Ethylenediamine tetramethylene phosphonic acid (EDTMPA), chloroplatinic acid hexahydrate ($H_2PtCl_6 \cdot 6H_2O$), SDS and sodium peroxide (NaOH) were obtained in Shanghai Macklin Biochemical Co., Ltd. Anhydrous ethanol, GA and sodium borohydride were purchased from Guangzhou Jinhuada Chemical Reagent Co., Ltd. SOx was obtained from J&K scientific company, 37 unit mg^{-1}. Sarcosine was obtained from the Acros organic company. Serum sample was purchased from Huayang Zhenglong Biochemical Products Research Office (Tianfu New District, Chengdu, Sichuan, China). All chemicals used were analytical reagents.

2.2. Instrumentations and measurements

Scanning electron microscopy (SEM) photographs were taken by Hitachi U70 electron microscope (Japan, acceleration voltage: 5 kV). Element Mapping was carried out by energy dispersive spectrometer (EDS, acceleration voltage: 15 kV). Nitrogen adsorption desorption data were measured by a Micromeritics 3Flex three-station full-function multi-purpose adsorption instrument (N_2, 77 K). Transmission electron microscope (TEM) image was taken by Tecnai G2 F30 (America, Thermo Fisher Scientific, acceleration voltage: 300 kV). X-ray electron diffraction (XRD) pattern was obtained by Rigaku MiniFlex 600 (Japan). Electrochemical experiments were carried out by a CHI 660C electrochemical workstation (Shanghai Chenhua Instrument Co., Ltd). A three electrodes systems were composed of a glassy carbon electrode (GCE, 3 mm in diameter) modified with SOx/Pt/MNP, a platinum wire and a saturated calomel electrode (SCE). All experiments were measured at room temperature (about 25 °C).

2.3. Synthesis of MNP and Pt/MNP

SDS (1.6 g), EDTMPA (0.436 g) and NaOH (0.32 g) were dissolved in deionized water (20 mL). Nickel sulfate hexahydrate (10.52 g) was dissolved in deionized water and added into the above solution, reacting 2 h. Subsequently, the mixture was transferred to an autoclave, ageing at 100 °C for 24 h. The pH of the mixture was adjusted to neutrality and dried at 50 °C to obtain MNP. Pt/MNP was synthesized by a simple method. MNP (3 g) was added into the ethanol solution of $H_2PtCl_6 \cdot 6H_2O$ (3 mL, 0.019 M) and stirred 24 h, afterward sodium borohydride dissolved with ethanol solution was added, stirring for 120 min. Finally, the mixture was put into a furnace at room temperature, and was heated at a heating rate of 5 °C min^{-1} and kept at 400 °C for 5 h to obtain Pt/MNP under N_2 atmosphere.

2.4. Preparation of sarcosine biosensor

The GCE was polished with alumina powder with a particle size of 1 and 0.3 μm. Pt/MNP (10 mg) was dispersed in deionized water (1 mL), and then the mixture was sonicated for 30 min to obtain black suspension. Pt/MNP suspension (10 μL) was covered on the surface of GCE to obtain Pt/MNP/GCE, drying at room temperature. SOx (5 μL, 4 unit μL^{-1}) was covered on the Pt/MNP/GCE, and then GA (10 μL, 0.1 M) was dropped and dried at room temperature to obtain SOx/Pt/MNP/GCE. The SOx/Pt/MNP/GCE was stored at 4 °C in phosphate buffer solution (PBS) when it was not used. All experiments were operated at room temperature.

3. Results and discussions

3.1. The morphology and structure of Pt/MNP

Morphology of Pt/MNP was observed by scanning electron microscope (acceleration voltage: 5 kV), as shown in Fig. 1 (a). There are numerous small three-dimensional holes on the surface of the material. The inset of Fig. 1 (a) is a magnified part of the surface,

Please cite this article in press as: Q. Wang, et al., Platinum-loaded mesoporous nickel phosphonate and its electrochemical application for sarcosine detection, Analytica Chimica Acta (2018), https://doi.org/10.1016/j.aca.2018.09.027

which displays piled hole with a diameter about 35 nm. Fig. 1 (b) is a nitrogen adsorption-desorption isotherm (N_2, 77 K). The inset shows its corresponding pore volume and pore size differential distribution curve. According to the regulation of nitrogen adsorption-desorption isothermal classified by the international union of pure and applied chemistry (IUPAC), the nitrogen adsorption-desorption isotherm of Fig. 1 (b) belongs to Class IV H3 isotherms [23,24]. Above the specific high pressure zone ($P / P_0 > 0.6$), a significant and nonparallel hysteresis loop is observed, which indicates that the material is stacked to form a slit hole. The Pt/MNP is calculated to own a surface area (BET) of 283 $m^2 g^{-1}$, average pore width (BJH) of 16.038 nm and pore volume (BJH) of 0.537 $cm^3 g^{-1}$. Fig. 1 (c) exhibits the TEM (acceleration voltage: 300 kV) image of Pt/MNP, it shows a mesoporous structure and many Pt particles are dispersed and loaded on the surface of MNP, which is consistent with Fig. 2 (a). From the inset of Fig. 1 (c), it can be clearly seen that the lattice is 0.223 nm, which presents the face-centered-cubic (FCC) of Pt lattice with (111) plane, corresponding to the result of XRD exhibited in Fig. 1 (d). Fig. 1 (d) displays XRD of Pt/MNP. There are four diffraction peaks at 39.89°, 46.2°, 67.68° and 81.21°, corresponding to the plane (111), (200), (220) and (311) of Pt respectively. The result of it demonstrates that pt particles exist in the composite.

Fig. 2 (a) displays an elemental distribution of Pt/MNP. Pt, N, C, Ni, P and O were characterized by elemental mapping. It clearly shows that Pt was evenly distributed over the MNP surface, which may be the reason why Pt/MNP has high catalytic activity. EDS's pattern of Pt/MNP is exhibited in Fig. 2 (b) and the inset shows their corresponding element mass fraction. The result of element content analysis demonstrates the element mass fraction of Pt is 13.94%, which also proves that Pt was successfully reduced.

3.2. Electrochemical characterization and amperometric response of the modified electrode

In 5 mM potassium ferricyanide solution, the CV curves of Pt/MNP/GCE at different scan rate (0.01, 0.02, 0.04, 0.06, 0.08, 0.1, 0.15 and 0.2 V s^{-1}) are presented in Fig. 3 (a). It can be observed from Fig. 3 (a) that the reduction peak and the oxidation peak are respectively corresponding at about 0.4 V and 0.5 V, indicating that this is a reversible redox process. As the scan rate increases, the peak potential shifted slightly toward a more positive direction. The inset of Fig. 3 (a) displays the corresponding relationship between peak current and the square root of scan rate ($v^{1/2}$). When the peak current displays a linear relationship with the square root of the scan rate, the reaction is a diffusion-controlled process. When the peak current is linearly associated with the scan rate, this is a surface-controlled reaction [25]. In our present work, it is a nice linear relationship between peak current and square root of scan rate ($v^{1/2}$). The correlation coefficient is 0.993 ($n = 8$) and 0.997

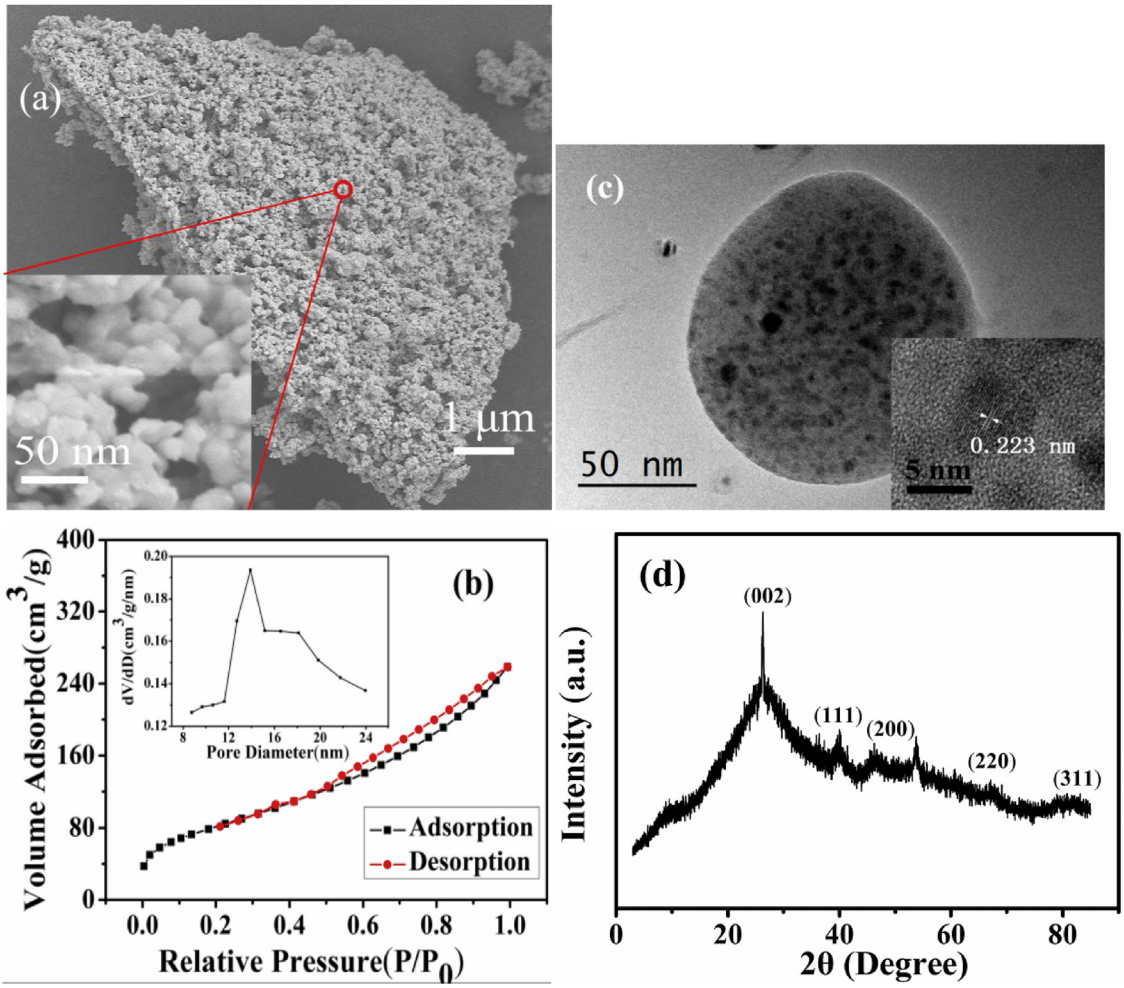

Fig. 1. (a) SEM image of Pt/MNP, the inset is partially magnified area; (b) Nitrogen adsorption-desorption isotherm of Pt/MNP. The inset shows its corresponding pore volume and pore size differential distribution curve; (c) TEM image of Pt/MNP. The inset shows the HRTEM image; (d) wide angle XRD of Pt/MNP.

Please cite this article in press as: Q. Wang, et al., Platinum-loaded mesoporous nickel phosphonate and its electrochemical application for sarcosine detection, Analytica Chimica Acta (2018), https://doi.org/10.1016/j.aca.2018.09.027

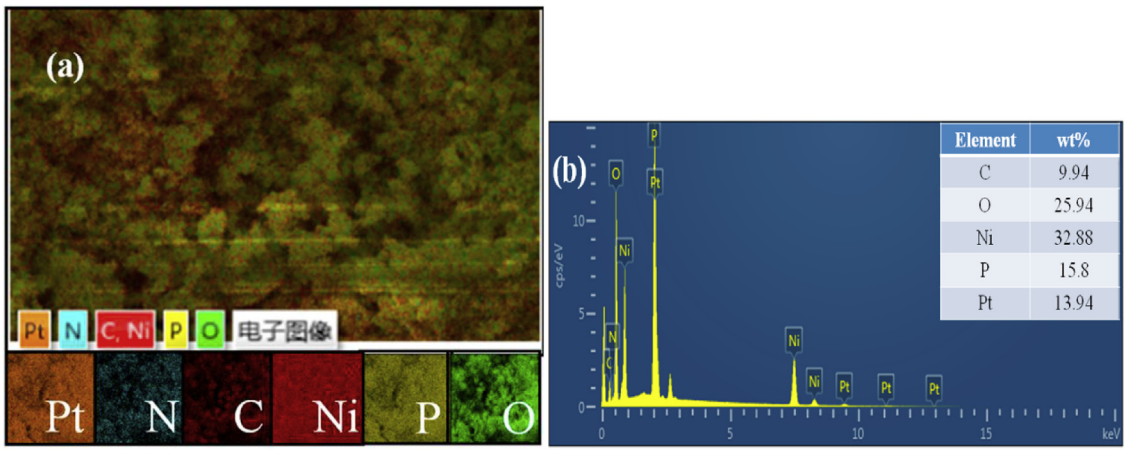

Fig. 2. (a) Elemental mapping analysis and (b) EDS dates of Pt/MNP.

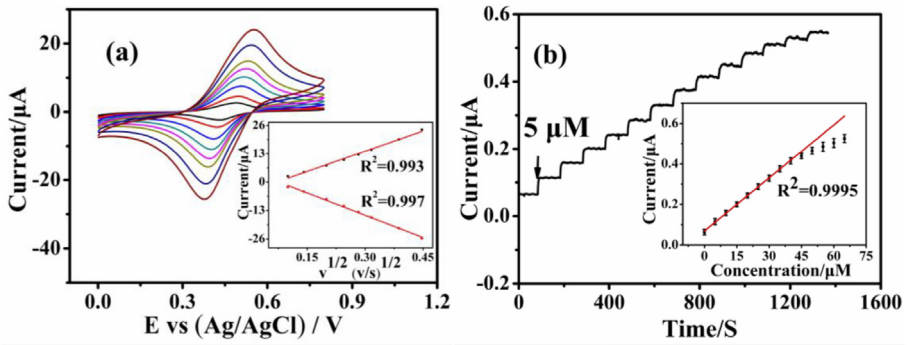

Fig. 3. (a) CV curves of Pt/MNP/GCE in 5 mM potassium ferricyanide solution at different scan rates (0.01, 0.02, 0.04, 0.06, 0.08, 0.1, 0.15 and 0.2 V s^{-1}). The inset shows the linear relationship between peak currents and the square root of scan rate ($v^{1/2}$); (b) The amperometric responses curve of SOx/Pt/MNP/GCE with successive injection of 5 μM sarcosine in PBS (applied potential: +0.4 V). The inset displays the corresponding I-C linear relationship.

(n = 8) respectively, which demonstrates that the kinetic of Pt/MNP/GCE was a diffusion-controlled process.

Fig. 3 (b) depicts the amperometric current curve of SOx/Pt/MNP/GCE with successively adding 10 μL of 5 mM sarcosine in 10 mL PBS (0.1 M, pH = 7.0) at +0.4 V with stirring. There is a great response when sarcosine was added. The inset of Fig. 3 (b) manifests the linear relationship between responsive current and sarcosine concentration. The linear range is 5–40 μM and the linear regression equation is as follows: I (μA) = 0.00873 $C_{sarcosine}$ (μM) + 0.06842 (R^2 = 0.9995, n = 14). The limit of detection (LOD) is estimated to be 0.24 μM (S/N = 3) and the sensitivity is 123.51 μA mM^{-1} cm^{-2}. The relevant parameters of amperometric sarcosine biosensors are exhibited in Table 1.

3.3. Interference test

Fig. 4 depicts interference experiment of SOx/Pt/MNP/GCE. Interference substance such as 0.1 M citric acid (CA), maltose, fructose, ascorbic acid (AA) and uric acid (UA) was successively added in 10 mL PBS (0.1 M, pH = 7.0) at +0.4 V with stirring, as shown in Fig. 4 (a). From Fig. 4 (b), it shows that CA, maltose and fructose have no interference with the detection of sarcosine. Only 5% and 5.5% of currents changed when 100 μM AA and UA were added into PBS. Compared to reference [16], the interference of AA is smaller. This phenomenon may be attributed to the reason as follows: firstly, Pt/MNP with mesoporous structure provides sufficient space for electrocatalysis oxidation reaction; secondly, the double-layered GA cross-linked membrane exhibits repellency to interference substance, which may limit the diffusion of interference substance.

3.4. Real sample test

In order to explore the application of SOx/Pt/MNP/GCE in physiological environment, we also have performed a titration method to detect sarcosine in a human serum sample, as shown in Fig. 5. Herein, 10 μM sarcosine is successively injected into human serum sample three times at +0.4 V and the concentration of

Table 1
The relevant parameter of some amperometric sarcosine biosensors.

Materials	Linear range (μM)	LOD (μM)	Applied potential (V vs. SCE)	Ref
SOx/PVA-Au-pphTEOS	500–7500	500	0.55	[26]
SOx/Pt@ZIF8/Nafion	5–30	1.06	0.4	[16]
SOx/carbon screen printed electrodes	0.01–0.1	0.016	0.6	[17]
SOx/Pt/MNP/GCE	5–40	0.24	0.4	This work

Please cite this article in press as: Q. Wang, et al., Platinum-loaded mesoporous nickel phosphonate and its electrochemical application for sarcosine detection, Analytica Chimica Acta (2018), https://doi.org/10.1016/j.aca.2018.09.027

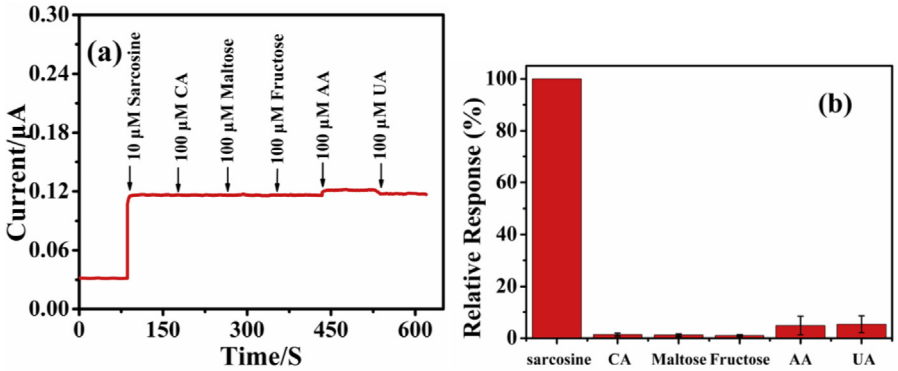

Fig. 4. (a) The amperometric curve of the SOx/Pt/MNP/GCE with successively adding 10 μL 0.01 M sarcosine and 0.1 M CA, Maltose, Fructose, AA, UA in PBS at +0.4 V; (b) analytical histogram of interference substance.

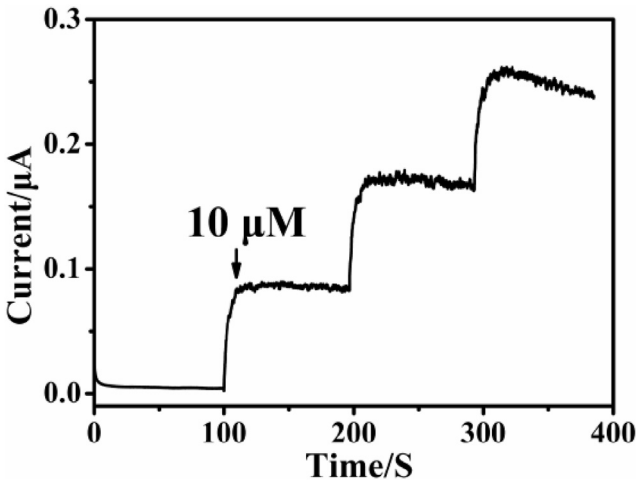

Fig. 5. Amperometric curve of SOx/Pt/MNP/GCE with successively adding 10 μM sarcosine (three times) in normal human serum at +0.4 V.

Table 2
Detection of sarcosine in normal human serum.

Sample	Add (μM)	Found (μM)	RSD %	Recovery %
Sarcosine	10	9.28	1.8	92.8
Sarcosine	20	18.90	1.5	94.5
Sarcosine	30	28.98	1.7	96.6

sarcosine in normal human serum is calculated using the linear relationship showing in Fig. 3 (b), the result is shown in Table 2. These results indicate that sarcosine biosensor based on Pt/MNP can be used to detect sarcosine in biological samples.

4. Conclusion

In summary, we have prepared Pt/MNP with a specific surface area of 283 $m^2 g^{-1}$ by a simple strategy and apply it to prepare a sarcosine biosensor to detect sarcosine. The mesoporous structure increases active sites, which make the biosensor exhibit higher electrochemical performance. The linear range, sensitivity and limit of detection of sarcosine biosensor are 5–40 μM, 123.51 μA $mM^{-1} cm^{-2}$ and 0.24 μM (S/N = 3), respectively. Additionally, the sarcosine biosensor based on Pt/MNP also shows an excellent performance in the anti-interference experiment. Therefore, it has lots of potential applications to develop electrochemical biosensor with good anti-interference performance.

Acknowledgement

The authors greatly appreciate the financial support from the Shenzhen Science and Technology Research grant (201886078).

References

[1] R.L. Siegel, K.D. Miller, A. Jemal, Cancer statistics, 2015, Ca-cancer J. Clin. 65 (2015) 5–29.
[2] R.L. Siegel, K.D. Miller, A. Jemal, Cancer statistics, 2016, Ca-cancer J. Clin. 66 (2016) 7–30.
[3] R.L. Siegel, K.D. Miller, A. Jemal, Cancer statistics, 2017, Ca-cancer J. Clin. 67 (2017) 7–30.
[4] W.Q. Chen, R.S. Zheng, P.D. Baade, S.W. Zhang, H.M. Zeng, F. Bray, A. Jemal, X.Q. Yu, J. He, Cancer statistics in China, 2015, Ca-cancer J. Clin. 66 (2016) 115–132.
[5] K. Hashimoto, T. Mizuno, H. Kitamura, T. Shindo, S. Takahashi, N. Masumori, The primary local stage at diagnosis predicts regional symptoms caused by local progression in patients with castration-resistant prostate cancer, Urology 85 (2015) 430–434.
[6] R. Raaijmakers, W.J. Kirkels, M.J. Roobol, M.F. Wildhagen, F.H. Schroder, Complication rates and risk factors of 5802 transrectal ultrasound-guided sextant biopsies of the prostate within a population-based screening program, Urology 60 (2002) 826–830.
[7] F.H. Schroeder, J. Hugosson, M.J. Roobol, T.L.J. Tammela, S. Ciatto, V. Nelen, M. Kwiatkowski, M. Lujan, H. Lilja, M. Zappa, L.J. Denis, F. Recker, A. Berenguer, L. Maattanen, C.H. Bangma, G. Aus, A. Villers, X. Rebillard, T. van der Kwast, B.G. Blijenberg, S.M. Moss, H.J. de Koning, A. Auvinen, E. Investigators, Screening and prostate-cancer mortality in a randomized European study, N. Engl. J. Med. 360 (2009) 1320–1328.
[8] H. Lilja, D. Ulmert, A.J. Vickers, Prostate-specific antigen and prostate cancer: prediction, detection and monitoring, Nat. Rev. Canc. 8 (2008) 268–278.
[9] I.M. Thompson, D.K. Pauler, P.J. Goodman, C.M. Tangen, M.S. Lucia, H.L. Parnes, L.M. Minasian, L.G. Ford, S.M. Lippman, E.D. Crawford, J.J. Crowley, C.A. Coltman, Prevalence of prostate cancer among men with a prostate-specific antigen level <= 4.0 ng per milliliter, N. Engl. J. Med. 350 (2004) 2239–2246.
[10] Y.Q. Jiang, X.L. Cheng, C.A. Wang, Y.F. Ma, Quantitative determination of sarcosine and related compounds in urinary samples by liquid chromatography with tandem mass spectrometry, Anal. Chem. 82 (2010) 9022–9027.
[11] A. Sreekumar, L.M. Poisson, T.M. Rajendiran, A.P. Khan, Q. Cao, J.D. Yu, B. Laxman, R. Mehra, R.J. Lonigro, Y. Li, M.K. Nyati, A. Ahsan, S. Kalyana-Sundaram, B. Han, X.H. Cao, J. Byun, G.S. Omenn, D. Ghosh, S. Pennathur, D.C. Alexander, A. Berger, J.R. Shuster, J.T. Wei, S. Varambally, C. Beecher, A.M. Chinnaiyan, Metabolomic profiles delineate potential role for sarcosine in prostate cancer progression, Nature 457 (2009) 910–914.
[12] I.M. Thompson, P.J. Goodman, C.M. Tangen, M.S. Lucia, G.J. Miller, L.G. Ford, M.M. Lieber, R.D. Cespedes, J.N. Atkins, S.M. Lippman, S.M. Carlin, A. Ryan, C.M. Szczepanek, J.J. Crowley, C.A. Coltman, The influence of finasteride on the development of prostate cancer, N. Engl. J. Med. 349 (2003) 215–224.
[13] T.E. Meyer, S.D. Fox, H.J. Issaq, X. Xu, L.W. Chu, T.D. Veenstra, A.W. Hsing, A reproducible and high-throughput HPLC/MS method to separate sarcosine from alpha- and beta-alanine and to quantify sarcosine in human serum and urine, Anal. Chem. 83 (2011) 5735–5740.
[14] Y.Z. Wang, S.Y. Ji, H.Y. Xu, W. Zhao, J.J. Xu, H.Y. Chen, Bidirectional electrochemiluminescence color switch: an application in detecting multimarkers of prostate cancer, Anal. Chem. 90 (2018) 3570–3575.
[15] N.N. Sun, B. Yan, A fluorescent probe based on a Tb3+/Cu2+ co-functionalized MOF for urinary sarcosine detection, Analyst 143 (2018) 2349–2355.

Please cite this article in press as: Q. Wang, et al., Platinum-loaded mesoporous nickel phosphonate and its electrochemical application for sarcosine detection, Analytica Chimica Acta (2018), https://doi.org/10.1016/j.aca.2018.09.027

[16] H.P. Yang, J.J. Wang, C. Yang, X.L. Zhao, S.H. Xie, Z.C. Ge, Nano Pt@ZIF8 modified electrode and its application to detect sarcosine, J. Electrochem. Soc. 165 (2018) H247–H250.
[17] T. Rebelo, C.M. Pereira, M.G.F. Sales, J.P. Noronha, J. Costa-Rodrigues, F. Silva, M.H. Fernandes, Sarcosine oxidase composite screen-printed electrode for sarcosine determination in biological samples, Anal. Chim. Acta 850 (2014) 26–32.
[18] X.Y. Jiang, L. Zhang, Y.L. Liu, X.D. Yu, Y.Y. Liang, P. Qu, W.W. Zhao, J.J. Xu, H.Y. Chen, Hierarchical CuInS2-based heterostructure: application for photocathodic bioanalysis of sarcosine, Biosens. Bioelectron. 107 (2018) 230–236.
[19] S.K. Maji, S. Sreejith, A.K. Mandal, X. Ma, Y.L. Zhao, Immobilizing gold nanoparticles in mesoporous silica covered reduced graphene oxide: a hybrid material for cancer cell detection through hydrogen peroxide sensing, ACS Appl. Mater. Interfaces 6 (2014) 13648–13656.
[20] C.X. Xu, F.L. Sun, H. Gao, J.P. Wang, Nanoporous platinum-cobalt alloy for electrochemical sensing for ethanol, hydrogen peroxide, and glucose, Anal. Chim. Acta 780 (2013) 20–27.
[21] Z.H. Bai, G.Y. Li, J.T. Liang, J. Su, Y. Zhang, H.Z. Chen, Y. Huang, W.G. Sui, Y.X. Zhao, Non-enzymatic electrochemical biosensor based on Pt NPs/RGO-CS-Fc nano-hybrids for the detection of hydrogen peroxide in living cells, Biosens. Bioelectron. 82 (2016) 185–194.
[22] Q.R. Shi, Y. Song, C.Z. Zhu, H.P. Yang, D. Du, Y.H. Lin, Mesoporous Pt nanotubes as a novel sensing platform for sensitive detection of intracellular hydrogen peroxide, ACS Appl. Mater. Interfaces 7 (2015) 24288–24295.
[23] K.S.W. Sing, D.H. Everett, R.A.W. Haul, L. Moscou, R.A. Pierotti, J. Rouquerol, T. Siemieniewska, Reporting physisorption data for gas solid systems with special reference to the determination of surface-area and porosity (recommendations 1984), Pure Appl. Chem. 57 (1985) 603–619.
[24] J. Rouquerol, D. Avnir, C.W. Fairbridge, D.H. Everett, J.H. Haynes, N. Pernicone, J.D.F. Ramsay, K.S.W. Sing, K.K. Unger, Recommendations for the characterization of porous solids, Pure Appl. Chem. 66 (1994) 1739–1758.
[25] H. Yang, G. Gao, F. Teng, W. Liu, S. Chen, Z. Ge, Nickel hydroxide nanoflowers for a nonenzymatic electrochemical glucose sensor, J. Electrochem. Soc. 161 (2014) B216–B219.
[26] U. Lad, G.M. Kale, R. Bryaskova, Sarcosine oxidase encapsulated polyvinyl alcohol-silica-AuNP hybrid films for sarcosine sensing electrochemical bioelectrode, J. Electrochem. Soc. 161 (2014) B98–B101.

Please cite this article in press as: Q. Wang, et al., Platinum-loaded mesoporous nickel phosphonate and its electrochemical application for sarcosine detection, Analytica Chimica Acta (2018), https://doi.org/10.1016/j.aca.2018.09.027